Trio GEF mediates RhoA activation downstream of Slit2 and coordinates telencephalic wiring

Stéphanie Backer1-2§, Ludmilla Lokmane3§, Camille Landragin1-2, Marie Deck3, Sonia Garel3 and Evelyne Bloch-Gallego1-2*

1- Institut Cochin, Université Paris Descartes, CNRS UMR 8104, Paris, France.

2- INSERM, U1016 – 24, rue du Faubourg Saint-Jacques 75014 Paris, France.

3- Institut de Biologie de l'Ecole Normale Supérieure (IBENS), Ecole Normale Supérieure, CNRS UMR8197, INSERM U1024, PSL research University 75005, Paris, France.

§ Both authors contributed equally to the work

* Author for correspondence: Evelyne Bloch-Gallego, evelyne.bloch-gallego@inserm.fr.

Key words: Trio GEF, RhoA, neuron, migration, Slit2, axon guidance, RhoGTPase, mouse, embryo, thalamocortical, corridor cells

SUMMARY STATEMENT

Our *ex/in vivo* observations bring the demonstration that Trio is a master-intergrator for factors guiding axonal growth and cell migration, and telencephalic wiring.

SUMMARY

Trio, a member of the Dbl family of guanine nucleotide exchange factors (GEFs), activates Rac1 downstream of Netrin-1/DCC signalling in axon outgrowth and guidance. While it has been proposed that Trio also activates RhoA, the putative upstream factors remain unknown. Here, we show that Slit2 induces Trio-dependent RhoA activation, revealing a crosstalk between Slit and Trio/RhoA signalling. Consistently, we found that RhoA activity is hindered *in vivo* in *trio* mutant mouse embryos. We next studied the development of the ventral telencephalon and thalamocortical axons, previously shown to be controlled by Slit2. Remarkably, this analysis revealed that *Trio* KO shows phenotypes that bear strong similarities to the ones reported in *Slit2* KO mice in both guidepost corridor cells and thalamocortical axon pathfinding in the ventral telencephalon. Taken together, our results show that Trio induces RhoA activation downstream of Slit2 and support a functional role in ensuring the proper positioning of both guidepost cells and a major axonal tract. Our study indicates a novel role for Trio in Slit2 signalling and forebrain wiring, thereby highlighting its role in multiple guidance pathways as well as in biological functions of importance for a factor involved in human brain disorders.

INTRODUCTION

The small GTPases (Rho guanosine triphosphatases) of the Rho family act as relays between the binding of extracellular signalling molecules and cytoskeleton remodeling to regulate events such as motility and axon outgrowth. Rho GTPases are molecular switches that mostly cycle between an inactive GDP-bound and an active GTP-bound state (Jaffe and Hall, 2005). The control of Rho GTPase nucleotide cycling is mainly performed by two types of regulatory proteins: guanine nucleotide exchange factors (GEFs) enhance the GTP-bound state whereas GTP hydrolysis is catalyzed by GTPase-activating proteins (Tcherkezian and Lamarche-Vane, 2007). We analyse here the role of Trio-GEF, a large protein of 350 kD that interestingly presents a peculiar structural feature, including two catalytic GEF domains that target small GTPases with apparent antagonistic downstream activities. The N-terminal Dbl-homology-Pleckstrin-homology (DH-PH) unit (TrioGEF1) mediates GDP to GTP exchange on Rac1 and RhoG whereas the C-terminal DH-PH unit (TrioGEF2) activates RhoA. Trio is highly expressed in the brain (Portales-Casamar et al., 2006). Recent findings have well established the signalling pathways that allow Trio to mediate Netrin-1/DCC signalling in axon outgrowth and guidance through the presence and functionality of the GEF1 domain and its ability to activate Rac1 (DeGeer et al., 2015). Neither using the whole protein *in vitro* (Bellanger et al., 1998; Blangy et al., 2000; Debant et al., 1996), nor in mammals *in vivo* has the role and functionality of the RhoA-GEF2 domain been demonstrated. No upstream signalling molecule has been proposed so far to bind Trio to subsequently activate RhoA.

We question here the role and partners of Trio in RhoA activation in mammals. RhoA activation downstream Slit has been proposed to be decisive in the context of repulsive events (Liu et al., 2012). We have investigated whether Trio could be a molecular integrator that could act *in vivo* as a GEF to activate RhoA upon a repulsive guidance cue. Slit2 was chosen as a candidate since it is able to modulate axon outgrowth and neuronal migration guidance. The phenotypic analysis of the development of the CNS in *trio* knockout (KO) has reported defects in axonal projections, in particular those that form the internal capsule (Briancon-Marjollet et al., 2008). Remarkably, a dramatic abnormal telencephalic phenotype has been reported in single *Slit2* KO mouse model (Bielle

et al., 2011). Thus, based on the detailed mis-wiring in *Slit2* KO, we have chosen to focus, in *trio* KO, on the development of thalamocortical axons (TCA) that occurs, in mouse, from E12 when they extend ventrally from the thalamus into the ventral telencephalon. Then, TCA turn dorsolaterally to cross the diencephalic-telencephalic boundary at E13, reach the internal capsule and fan out before reaching their appropriate cortical region around E16. Their outgrowth across the subpallium requires the presence of guidepost neurons organized as a corridor and called "corridor cells" (Lopez-Bendito et al., 2006). Corridor cells originate in the lateral ganglionic eminence (LGE) and migrate tangentially in the medial ganglionic eminence (MGE). Slit2 has the property to orient guidepost neurons migratory path and consequently the path of TCA (Bielle et al., 2011).

We show here that *ex vivo*, the signalling pathway downstream Slit2 activates RhoA but is impaired in the absence of Trio in Mouse Embryonic Fibroblasts (MEFs) that have been freshly obtained from control or mutant embryos out of *trio*$^{+/-}$ littermates. In addition, *in vivo*, the absence of Trio hinders both RhoA and Rac1 activities in the ventral telencephalon in *trio* KO. Remarkably, the analysis of the phenotype of *trio* KO reveals that guidepost corridor cells are mispositioned from E12, and thalamocortical axons (TCA) show i) an aberrant pathfinding for some of them and ii) a massive disorganization with fasciculated bundles in the ventral telencephalon which would result from corridor mispositioning, altogether with misintegration of Slit2 guidance cue by TCA along their pathway. Thus we describe here the sequence responsible for abnormal telencephalic development in *trio* mutant mice, with an involvement of Trio both in positioning migrating corridor cells and in guiding TCA pathfinding. Our results demonstrate Trio as a master-integrator for Slit signalling and RhoA activation, in addition to the previously demonstrated Netrin-1/DCC/Rac1 signalling. Therefore Trio appears as a bottleneck for transducing guidance cues and cytoskeleton remodeling in the processes of both axon outgrowth/pathfinding and neuronal migration during embryonic development of the rostral CNS.

RESULTS

RhoA activity is severely decreased in MEFs derived from *trio*$^{-/-}$ embryos

To decipher the role of Trio in mediating repulsion in response to guidance cues in mammals, we investigated the possible link between Slit/Robo and Trio/RhoA pathways. Recent data from genetics of Drosophila have suggested that repulsion by Robo involves Trio activity (Long et al., 2016). A role for Trio-mediated RhoA activation has been shown in the eye development of chick embryos (Plageman et al., 2011) and was also proposed to affect the innate immune response in *C. elegans* (McMullan et al., 2012).

We thus analysed the level of RhoA activity in control or Slit2-treated Mouse Embryonic Fibroblasts (MEFs) freshly dissociated from control or *trio* KO E14-E18 embryos (Fig. 1A). We first ensured that Trio was properly expressed in control MEFs extracts (Fig. S1A). Trio can encode several isoforms as a result of alternative splicing. In control MEFs extracts, Trio antibodies mainly detect a doublet that likely corresponds to Trio D (300kDa) and Trio A (250kDa), two splice variants previously reported to be expressed in the central nervous system (Schmidt and Debant, 2014). Although faint, the full-length form of Trio (migrating at around 350kDa) was also detected (Fig. S1A, left panels). None of these Trio isoforms could be detected in *trio*$^{-/-}$ MEFs. We also ensured that both control and *trio*$^{-/-}$ MEFs properly express Robo1/2 receptors (Fig. S1A, right panels).

Prior to Slit2 stimulation, the basal level of RhoA activation was comparable in both wt and *trio* KO MEFs (Fig. 1A, upper left panels). In wild type MEFs, Slit2 treatment led to a transient increase of RhoA GTP level: a significant stimulation was detected after 5 min of treatment (**; $p<0.001$), whereas no more stimulation was observed after 15 min. In contrast, no increase of RhoA activation was observed in *trio*$^{-/-}$ MEFs (Fig. 1A, upper right panel). This indicates that the transient activation of RhoA upon Slit2 stimulation observed in control MEFs is dependent on the presence of Trio.

Since Trio was previously shown to be able to activate Rac1 in response to Netrin-1 (Briancon-Marjollet et al., 2008), we investigated whether Slit2 could activate Rac1 in a Trio-dependent manner in MEFs. We therefore analysed the rate of Rac1 activation upon Slit2 stimulation of wt and *trio*$^{-/-}$ MEFs (Fig. 1A, bottom panels). While the rate of Rac1 activation after a 5-min Slit2 treatment was

low in control MEFs, it increased significantly after Slit2 stimulation of *trio*$^{-/-}$ MEFs (**; p<0.001). This assay thus revealed that the absence of Trio, instead of preventing Rac1 activation in response to Slit, induces or facilitates its activation. These data show that the presence of Trio is required for RhoA activation after Slit2 stimulation but antagonizes Rac1 activation, illustrating a possible physiological Rho-Rac antagonism that could involve Trio-GEF (see Discussion).

Trio is expressed in the ventral telencephalon and thalamic region during development and it regulates RhoA activity *in vivo*

We next aimed to determine whether Trio modulates RhoA activity *in vivo*. Therefore, we first examined whether Trio shows a specific transcript expression in the embryonic brain, by performing *in situ* hybridization from E12.5 to birth (Fig. 2). We observed a very broad expression in the neocortex (NCx) and ventral telencephalon mantle at E12.5 (Fig. 2A, B). The labelling was detected in the mantle layer (Mtl) of both LGE (Lateral Ganglionic Eminence) and MGE (Medial Ganglionic Eminence) but quite low in their ventricular and subventricular zones (asterisks). *Trio* transcripts were also detected in striatum (Str), diagonal and preoptic zones (POA) whereas its expression is low rostrally in the pallium (not shown). At E14.5 (Fig. 2C, D), *Trio* was strongly expressed in the thalamus (Th) and in the ventral part of the telencephalon (Fig. 2C) as well as in the neocortex cortical plate (CP). At birth (P0, Fig. 2E, F), *Trio* transcripts were present in the striatum (Str), hippocampus (Hip), and neocortex (NCx). In the hippocampus, CA subiculum, the dorsolateral part of the pre/parasubiculum and the adjacent region of the cingular anterior and infralimbic cortex express *Trio*. Notably, *in situ* hybridization probes including the full-length *Trio* transcripts or restricted to the GEF-2 domain (present in all Trio isoforms except Trio B and C, (Schmidt and Debant, 2014) showed a similar expression pattern. Consistent with these ISH data, Western blot analyses detected the Trio protein in the ventral telencephalon, the ganglionic eminences and the thalamus. All three tissues mainly expressed Trio D (300kDa) and Trio A (250kDa) isoforms but very low levels of full-length Trio (Fig. 1B, left panel).

We thus focused our functional studies on the ventral telencephalon, a structure previously shown to be perturbed in *trio* KO (Briancon-Marjollet et al., 2008) and to be responsive to Slit2 signalling (Bielle et al., 2011). Pull-down assays using whole ventral telencephalon extracts at E14.5, revealed a more than 2-fold decrease in activated/total RhoA ratio in *trio*$^{-/-}$ compared to wild type extracts (n=4 independent experiments, p=0.02 Fig. 1B). Attempts to further stimulate RhoA activity with Slit2 on dilacerated telencephalon were not successful, possibly due to technical aspects or to a constitutive activation by endogenous Slit2. Nevertheless, together with our *ex-vivo* data, revealing the lack of RhoA stimulation upon Slit activation in *trio*$^{-/-}$ MEFs, this endogenous decrease in active (GTP-bound) RhoA in the absence of Trio is consistent with a role of Trio in RhoA activation downstream Slit2 *in vivo.*

Netrin-1, Slits and Robo receptors remain properly expressed in the absence of Trio

Since Rho has been linked to the transcriptional machinery through the Rho-SRF connection (Settleman, 2003), we ensured that the absence of Trio, that affects Rho activation in the telencephalon (Fig. 1B), does not affect cell synthesis of guidance cues. At E14.5, ISH with both *Slit2* or *Netrin-1* probes have been performed in control and *trio*$^{-/-}$ mutants. In the absence of *trio* (Fig. 3E), Netrin-1 remains expressed as previously reported and illustrated in wild type animals here (Fig. 3A), i.e. in the ventricular zone of the LGE, in the whole striatum and in the most basal part of the telencephalon, including the globus pallidus (GP). *Slit2* also remains similarly expressed in both wild type (Fig. 3B, B') and *trio*$^{-/-}$ (Fig. 3 F, F') mice, both in localization and intensity, ie at a high level in the ventral midline. The expression domains of *Robo* receptors remain roughly identical in control (C and D for *Robo1* and *Robo2* respectively) and mutant *trio*$^{-/-}$ (G and H for *Robo1* and *Robo2* respectively) in thalamic (not illustrated) and telencephalic regions. In both control and mutant embryos, *Robo1* and *Robo2* transcripts are expressed in a partially complementary manner in the thalamus, and both receptors are expressed in the striatum. *Robo2* labeling is intense and localized in the striatal region while the one of *Robo1* shows a more diffuse aspect in the mantle zone. *Robo1* expression is further assessed by western blot, in E13 cortical and thalamic extracts, and in ventral telencephalon extracts at E14 (Fig. S1B).

Corridor guidepost cells show a defective positioning

Because our data suggested that Trio acts downstream of Slit2 *in vivo,* we next compared the phenotypes of *trio* KO to the ones reported in *Slit2* KO mice (Bielle et al., 2011). In particular, Slit2 had been demonstrated to be required for proper development of the telencephalon, notably corridor cells positioning (Lopez-Bendito et al., 2006) (Bielle et al., 2011).

Corridor cells migrate tangentially from the LGE at E12 into the MGE, and allow the path of TCA at E13.5 (Lopez-Bendito et al., 2006). Corridor cells were visualized with an *Ebf1 in situ* hybridization probe that also labels the striatum (Fig. 4). From E12.5 (n=2), in mutant mice (Fig. 4B), *Ebf1*-expressing cells formed an abnormal horizontal "beak", which contrasts with the continuous appearance of the migratory stream in wild type embryos (Fig. 4A). At E14.5 (n=5), the geometry of *Ebf1*-positive corridor between the LGE and MGE was still strikingly compacted in mutant mice, with some cells mis-oriented towards the MGE instead of migrating more ventrally (Fig. 4D), compared to the regular organization observed in control embryos of the same stage (Fig. 4C). Striatal defects were also observed at E18.5 (n=3; not shown). Interestingly, the corridor was similarly distorted and oriented towards the midline in *Slit2* KO (Bielle et al., 2011). Altogether, these phenotypic observations in *trio* mutant mice reveal that the positioning of corridor cells is impaired, which could affect the TCA navigation as reported in *Slit2* KO (Bielle et al., 2011).

Abnormal outgrowth and pathfinding of thalamocortical axons in *trio* KO

Invasion of the striatum and cortex by TCA depends on corridor cells positioning and has been reported to be delayed in *Slit2* KO (Bielle et al., 2011) – whereas it is premature in *Robo1* KO (Bielle et al., 2011). We thus analysed TCA pathfinding using both immunostaining and axonal tracing by carbocyanines injections. To analyse the development of axons, L1 immunoreactivity has been used to visualize thalamocortical fibers. At E14.5, in *trio* mutants (n=5) TCA seemed to have a delayed outgrowth through the striatum and showed misguided bundles. A part of axons were stalled ventrally in the mutant ventral telencephalon (Fig. 5E) whereas in controls (n=5), TCA had already crossed this structure and reached the neocortex (Fig. 5A). Analysis of TCA at E18.5 using L1 immunostaining

(n=3; Fig. 5I, M) revealed that axons had reached the neocortex in *trio* mutants (Fig. 5M) but they were forming disorganized bundles across the striatum, in contrast to their fan shape in control animals (Fig. 5I). Thus TCA outgrowth and trajectory were impaired between E14.5 and E18.5 in the absence of Trio.

The proper pathfinding of TCA when they emerge from the thalamus and navigate through the internal capsule regulates their initial addressing to neocortical regions (Lokmane et al., 2013). We thus further analysed the respective pathways of motor and somatosensory TCA, originating from the ventro-lateral thalamus (VL) and the ventro-posterior (VP) nuclei, respectively (Lokmane and Garel, 2014). At E16.5, anterograde tracings by double DiI and DiA injections in the VP and VL nuclei respectively show that TCA organization is severely impaired in mutants (n= 3; Fig. 5F-H). Indeed, in controls (n=3; Fig. 5B-D) VL motor and VP somatosensory TCA reached the neocortex with a strereotyped compact trajectory through the ventral telencephalon: VL axons (DiA in green) were more dorsal in the internal capsule than the VP TCA (DiI in red). In *trio* mutants, VP somatosensory axons (in red, compare Fig. 5F-H with Fig. 5B-D) progressed as a larger and disorganized bundle when crossing the ventral telencephalon, albeit some axons succeded in reaching the neocortex at E16.5. In contrast, motor projections that arose from the VL nucleus (VL in green, compare Fig. 5F-H with Fig. 5B-D) avoided crossing the ventral telencephalon and remained blocked caudally in the ventral telecenphalon and did not reach the neocortex.

Finally, by retrograde tracing at E18.5 after double injections of DiA in motor (M1) and DiI in somatosensory (S1) neocortex (Fig. 5J-L and N-P), we monitored the topographic projections of TCA. In wild type animals, double injections clearly show the stereotyped exclusive path of motor and somatosensory axons through the ventral telencephalon as well as the retrolabelling of thalamic neurons in specific nuclei (n=5; Fig. 5J-L). In mutant embryos (n=3, Fig. 5N-P), DiI injections in S1 led to a retrolabelling in the thalamus indicating that TCA did reach S1. Furthermore, axonal labelling in the ventral telencephalon revealed that like at E16.5, somatosensory TCA are disorganized at E18.5. In the mutant, DiA injections in M1 show an axonal labelling in the dorsal striatum but not in the internal capsule nor in the thalamus. The variation in the dispersion of the thalamic axonal tract,

quantified in either wild type or *trio*$^{-/-}$ mutant embryos, reflects the disorganized outgrowth and guidance of TCA, less constrained in the absence of Trio (Fig. 5Q).

Our analyses thus indicate that i) the trajectory of growing TCA is affected when they reach the ventral telencephalon, showing delayed outgrowth and enlarged fascicles in the absence of *trio*; ii) some somatosensory TCA reached the neocortex via aberrant and ectopic pathways in *trio* mutants, whereas motor TCA were more severely affected and did not reach the neocortex.

Impaired collapse responses to Slit2 in dissociated thalamic neurons from *trio* KO

To further analyse the functional link between Slit2 signalling and Trio function, we performed collapse assays by treating E13.5 dissociated thalamic neurons from either wt (n=5, Fig. 6A-F) or *trio* mutant (n=6, Fig. 6G-L) embryos from 3 different littermates with Slit2 (Fig. 6). We therefore scored the number of collapsed versus non-collapsed thalamic axons growth cones, either without stimulation (wild type, n=403 and *trio*$^{-/-}$, n=419) or 20 minute after Slit2 stimulation (wild type, n=395 and *trio* $^{-/-}$, n= 354). The rate of collapsed growth cones (25%) in *trio* $^{-/-}$ thalamic axons is higher than in wild type (17%) in basal conditions without stimulation ($p<0.008$; **). Nevertheless, while Slit2 treatment induced a two-fold increase of collapsed growth cones from wild type thalamic neurons (16 to 35% collapse; $p<0.0001$ (****), Fig. 6M), the ratio of collapsed growth cones was not significantly increased (ns) in *trio* $^{-/-}$ thalamic axons (29% after Slit2 treatment versus 24% in basal conditions). These results indicated that in the absence of Trio, growth cones have lost their ability to collapse in response to Slit2. Thus, Trio seems to be important to mediate Slit2 driven growth cone collapse.

In conclusion, our detailed anatomical analysis of *trio*$^{-/-}$ mutants showed that, although not strictly identical in extent, *Trio* phenotypes is coherent and correlates with several striking observations previously reported in *Slit2* KO. In addition, the efficiency of Slit2 treatment for inducing growth cones collapse on dissociated thalamic neurons strongly depends on the presence of Trio. Finally, RhoA is activated upon Slit2 treatment in wild type MEFs but not in *trio*$^{-/-}$ MEFs. Thereby, both *in vivo* and *in vitro* assays strengthen the possibility that Trio, in addition to its established function downstream of Netrin-1, interacts with Slit2 signalling.

DISCUSSION

This work participates in filling in the missing links that surround Trio in the network of molecular interactions that control RhoA activation and it also demonstrates a crucial role of Trio downstream of Slit2. We report here that RhoA activity is increased upon Slit2 in a Trio dependent manner. *In vitro* and *in vivo*, RhoA activity is impaired in the absence of Trio. In addition, the collapsing activity of Slit2 on TCA is lost in the absence of Trio. Thus, we demonstrate here that Trio belongs to a signalling cascade downstream the guidance cue Slit2 that can induce RhoA activation *in vivo*. The development of the forebrain, in particular the development of the ventral telencephalon and TCA, were previously shown to be controlled by Slit2 and we have analysed these structures in *trio* mutants. The phenotype we observe in *trio* mutants is similar to the one reported by us and others in *Slit2* mutants (Bielle et al., 2011) in the following points: i) TCA are ventrally misrouted at the telencephalic/diencephalic boundary; ii) TCA have an abnormal ventral route through the telencephalon; iii) TCA that reach the neocortex show topographic defects; iv) the positioning of corridor cells is abnormal, which could be at least partly responsible for the defects in TCA outgrowth, guidance, and projections.

It is noteworthy that *Netrin1* or *DCC* mutants did not show a ventral misrouting of TCA nor defects in corridor cell positioning (Bielle et al., 2011; Braisted et al., 2000; Castillo-Paterna et al., 2015; Powell et al., 2008). They showed a difference in the speed of TCA progression and minor topographic organization defects, which is in sharp contrast with the profound abnormalities observed in *trio* KO.

Taken together, our results indicate that the phenotype observed in *trio* mutants shows striking similarities to the ones observed in *Slit2* mutants, and is much more severe than the one observed in *Netrin1/DCC* KOs. As such, our results support a potential role for Trio downstream Slit2 in this system.

Thus we report a major and novel role of Trio to ensure the signalling pathway downstream of Slit2 and the proper wiring of the telencephalon by guiding both corridor cells positioning and TCA pathfinding. In this integrative developmental process, Trio would confer the positional guidance information necessary for neuronal positioning and axon ordering to the cytoskeleton, required for the proper adult cytoarchitecture.

So far, Trio had been mainly studied and proposed to act downstream Netrin-1 (Schmidt and Debant, 2014), and it has been shown to mediate Rac1 activation and axon outgrowth and guidance in response to Netrin-1 (Briancon-Marjollet et al., 2008). Furthermore, along with Netrin-1/DCC/Trio signalling pathway, the phosphorylation of Trio has been reported to be essential for Rac1 activation by Netrin-1 and for the proper targeting of DCC to the cell surface of growth cones, in order to mediate Netrin-1-induced axon outgrowth (DeGeer et al., 2013). The present study demonstrates that Trio also participates in an additional signalling pathway including Slit/(Robo)/Trio/RhoA. Future studies will however be required to determine whether this pathway directly involves Robo and its intracellular domain binding to Trio upon stimulation by Slit2. Robo1/2 may not be the unique Trio partner downstream of Slit2 (Fig. 7).

Our results also show that RhoA – and not Rac1 - stimulation by Slit2 is strictly Trio dependent, whereas on the contrary, a very significant Rac1 activation by Slit2 only occurs in cells devoided of Trio-GEF activity. Trio thus seems to be involved in the regulation of a possible physiological Rho-Rac antagonism. Interestingly, the modifications of the growth cones shape result, among others, from variations of Rho and Rac activities. We report here that the rate of collapsed growth cones in *trio* $^{-/-}$ thalamic axons is higher than in wild type in basal conditions *in vitro* (Fig. 6), suggesting that Trio may be necessary to prevent some spontaneous thalamic growth cone collapse. Thus Trio may act as a mediator between RhoA and Rac1 pathway to promote the reciprocal inhibitory relationship between both GTPases, as previously deciphered for a class of GTPase-activating proteins, FilGAPs (Nakamura, 2013).

A recent literature has now well established that extracellular interactions and cross-talks between various guidance cues are required to direct axon guidance and neuronal migration during embryonic development. However, the signalling pathways that allow the integration of their respective or combined effects to reorganize the cytoskeleton remain poorly characterized. We reveal here that Trio can activate RhoA *in vivo* downstream Slit2 and could act as a molecular bottleneck to integrate both Rho and Rac signalling downstream Slit2 and Netrin-1 respectively.

RhoA activation downstream Slit has been proposed to be decisive in the context of repulsive events. It is in particular the case for the dispersion of oligodendrocyte precursors (Liu et al., 2012). We report here that Trio is strictly required to activate RhoA downstream Slit2 stimulation in MEFs and *in vivo*. Activation of the Rho GTPases Rac and Cdc42 promotes the formation of lamellipodia and filopodia respectively (Lawson and Burridge, 2014), whereas activation of the Rho family member RhoA leads to increased actomyosin contractility, growth cone collapse or cell dispersion. Thus, Rac and Cdc42 activation would mimick attractive axon guidance cues, while Rac and Cdc42 inhibition or RhoA activation mimicks repulsive cues, and Trio could mediate the effects of repulsive cues. Trio/RhoA is required for neuronal positioning of guidepost cells in response to Slit2, which ensures TCA outgrowth (as schematized in Fig. 7). The precise effect of Slit2 on corridor positioning remains to be analysed, possibly affecting their oriented migration or the efficiency of their migration.

It will be interesting to determine the specific functional domains of Trio that are involved and regulated during the respective activation of both Rac1 and RhoA and allow Trio to integrate signalling of different guidance cues to remodel the cytoskeleton. It is admitted that RhoGEF can be regulated by protein-protein or intramolecular interactions. Their activity can also be dependent on their subcellular localization, either membrane targeted or nuclear sequestrated (Cherfils and Zeghouf, 2013). *In vivo*, it would be interesting to define ultrastructurally conformational changes of Trio that can occur in the growth cone leading processes and in cell bodies, which could allow the accessibility and activity of either GEF1 and /or GEF2.

Other GTPases regulators of the actin cytoskeleton have been studied for their inhibitory action on small Rho GTPases (Rac1, RhoA, Cdc42) downstream of Slit. Slit–Robo GTPase activating proteins (srGAP1,2,3) were identified in a two-hybrid screen as downstream components of the Slit/Robo pathway in forebrain neuroblasts, and Rac1 inhibition has been proposed as a major consequence of sr-GAP recruitment. SrGAP3/MEGAP is a member of the Slit-Robo GAP (srGAP) family and is implicated in repulsive axon guidance and neuronal migration through Slit-Robo-mediated signal transduction. It has been shown to be part of the Slit-Robo pathway regulating neuronal migration and axonal branching (Wong et al., 2001). Anyway, although still to be demonstrated, Slit2 effects are at least partly linked to Cdc42 inactivation by srGAP1. In the context of guidance cues and to reconcile our observations and these results, it is plausible that either GAPs or GEFs lead to a specific balance of activity to modulate Rho GTPases, GEF specificity resulting also from their localization and from the presence of appropriate molecular partners.

The phenotypic analyses of *trio* mutants demonstrate that the loss of Trio signalling leads to an abnormal TCA navigation and defective wiring of the neocortex, suggesting a crucial role of Trio in orchestrating both guidepost cells migration, TCA outgrowth and somatotopic cortical projections. Trio seems to be involved both in wiring motor and somatosensory projections. Moreover the anterior commissure has been reported to be absent in *trio*-null embryos, and Netrin-1/DCC-dependent axonal projections that form the corpus callosum have also been reported to be defective in the mutants (Briancon-Marjollet et al., 2008). We have also observed that the lateral olfactory tract (LOT) is abnormally shaped in the absence of Trio and the pathfinding of the LOT is impaired in the mutant compared to the control (not illustrated). It is remarkable that the LOT proper development is similarly a function of the prior proper positioning of guide cells (LOT cells) and it involves the Slit/Robo pathway (Fouquet et al., 2007; Nguyen-Ba-Charvet et al., 2002). We suggest that Trio is an appropriate master integrator to regulate both tangential migration and axon outgrowth *in vivo* during mouse embryogenesis. We had previously shown that neuronal migration depends on the Rho/ROCK pathway while axon outgrowth depends on Rac1 activation (Causeret et al., 2004). Thus Trio could regulate axon outgrowth and neuronal migration through both its functional GEF domains.

Interestingly, Trio has been recently marked as a candidate gene for intellectual disability (ID) since four truncating monoallelic mutations have been identified in patients reported with mild to borderline ID combined with behavioral problems (Ba et al., 2016). It is noteworthy that heterozygous nonsense mutations have been reported in humans. Although recorded with intellectual disability, clinical exams also reveal motor deficits. In addition to *trio* mutations in cases of intellectual disability with both cognitive and motor defects, novel *de novo* genetic damage to both GEF domains that altered Trio catalytic activity have been recently proposed to contribute to neurodevelopmental diseases (ADS, schizophrenia, bipolar disease and intellectual disability) (Katrancha et al., 2017); (Sadybekov et al., 2017). Combining this report and our observations, it will be interesting to determine whether these patients carrying *trio* mutations show thalamic malformations or defective forebrain wiring, with impaired thalamocortical or reciprocal corticothalamic connections (Ba et al., 2016). It will also be of interest to investigate whether mono allelic mutations in either *slit/robo/Trio* could lead to similar syndroms, affecting a common signalling pathway, by targeted sequencing of Slit1/2, and Robo1/2 in over 2300 individuals previously revealed with ID.

In parallel, it will be worth testing whether heterozygous mice carrying a monoallelic *trio* mutation develop sensory or motor inabilities.

Remarkably, abnormal neuronal apoptosis has been reported in cases of mental retardation and/or lissencephaly (Di Donato et al., 2016). Our preliminary data reveal that apoptotic figures are rare events in the developing CNS devoided of Trio, but caspase positive areas have been detected between E15.5 and birth in thalamic nuclei - none in the ventral telencephalon. Note that despite anatomic misorganizations in the hindbrain (Backer et al., 2007) and spinal cord, no apoptotic figures were reported. Whether wiring defects in the absence of *trio* may lead to apoptosis remains to be characterized.

Taken together, our data demonstrate a novel role for Trio acting downstream of Slit2 and activating RhoA. These results strongly suggest that Trio can act as a molecular integrator of complementary positional and guidance information to allow axon ordering during embryogenesis, and to control the formation of topographic map in particular in the mature forebrain.

MATERIALS AND METHODS

Animals

Pregnant Swiss mice were purchased from Janvier Laboratories (Le Genest St Isle, France). Timed matings of *trio* $^{+/-}$ mice (O'Brien et al., 2000); BALB/c genetic background) were used to obtain embryos at different developmental stages. The day of vaginal plug was considered E0.5. DNA was isolated from the tail and used for genotyping with appropriate primers. Animals were handled in accordance with European regulations and the local ethics committee.

Fixation

Mouse embryos were obtained from timed mating of outbred Swiss mice (Janvier, Le Chesnet Saint Isle, France), or from heterozygous *trio* mutant mice (O'Brien et al., 2000). Mouse embryo between E12.5 and E15.5 were fixed by immersion with 4% paraformaldehyde solution (PFA), in phosphate buffer saline (PBS), pH 7.4, for 4 hours at 4°C; between E15.5 and E18.5 days, embryos were perfused and postfixed 6 hours with the same fixative. The brains were dissected out and cryoprotected according to Bloch-Gallego et al. (Bloch-Gallego et al., 1999). The frontal sections (20 µm thick) were collected using a cryostat on parallel sets of SuperFrost Plus slides and stored at –80ºC until use.

Isolation of MEFs from *trio*$^{+/-}$ littermates

MEFs could be prepared from E14.5 and E18.5 using the eviscerated individual embryo freed of blood vessels or the skin of the back for older embryos. Tissues were trypsinised (0.25%) at 37° for one hour, dissociated and centrifuged quickly. The supernatant was collected and seeded in DMEM (Life Technologies)/10% fetal calf serum, 1% penicillin/ streptomycin (100 UI/ml), while the pellet was trypsinized one hour more. The previous steps were repeated until most tissues were dissociated.

Primary cultures of E13 thalamic neurons

Coronal slices of different levels of wt and *trio*$^{-/-}$ mouse at embryonic day E13.5 were prepared as previously described by Lopez-bendito et al., 2006. Thalamic tissues were dissected from these slices, dissociated by trypsin-EDTA 0, 05% (Invitrogen) for 15 minutes at 37°C and cultured on poly-L-ornithine/laminin (both from Sigma Aldrich, St. Louis, MO, USA) coated wells in neurobasal medium supplemented with B27 1x, N2 1x (both from Gibco, Fisher Scientific), 20 mM glucose (Sigma-Aldrich, St. Louis, MO, USA), 2 mM glutamine, and penicillin-streptomycin 1x (both from Invitrogen, Carlsbad, CA, USA) for 24-36 h.

Collapse assay

Dissociated cultures from thalamic neurons at E13.5 were performed as described in (Deck et al., 2013). After 24 hrs of culture, neurons were incubated with commercial mouse-Slit2 at a 2µg/ml final concentration (R&D Systems Europe) for 20 min at 37°C, fixed, immunostained with mouse anti-ß-tubulin antibody (Tuj1, 1:200, Sigma-Aldrich), and labeled with Texas Red-X or Alexa Fluor 488-Phalloidin (1 :200, Molecular Probes, ThermoFisher Scientific) to analyse growth cone morphologies. Collapsed growth cones were scored as in (Castellani et al., 2000).

Immunohistochemistry and antibodies

Immunochemistry was performed on vibratome sections. After fixation, the brains were dissected out, embedded in agarose 4% in PBS and cut into 100 mm thick sections with a vibratome. Free floating sections were saturated in PBS, 10% FCS, 0,1 % triton. The immunostaining was performed with rat anti-L1 1:200 (Millipore) overnight at room temperature. The primary antibody was revealed using secondary anti-rat antibody conjugated to Alexa 488 or 546 (1:1000; Life technologies). Once the immunoreactions performed, the sections were treated with DAPI (1 mg/ml; Vector).

In situ hybridization and RNA probes

In situ hybridization (ISH) was performed on 20 µm thick cryosections according to Bloch-Gallego et al. (Bloch-Gallego et al., 1999). We linearized the mouse *trio* subclone (MT7 for all *trio* isoforms, Backer et al., 2007) with *NotI* (Invitrogen) enzymes and used T7 RNA polymerase (Roche). We synthesized from mouse E14 telencephalon cDNA, a probe corresponding to the trio-GEF2 domain using the following primers - Forward AGGCACTATGTTTTGCAAGAG and reverse CCACGTTTGCCGGACGCT – altogether with the T7 polymerase by RT-PCR. We linearized the mouse *ebf1* subclone with *Xba1* (Invitrogen) enzymes and used T3 RNA polymerase (Bielle et al., 2011).

Dosage of the endogenous RhoA or Rac1 activity in ventral telencephalic explants or MEFs

Freshly dissected ventral telencephalon or MEFs were lysed with ice cold lysis buffer (25 mM Tris pH 7.5, 1% NP40, 100 mM NaCl, 10mM MgCl2, 5% glycerol, 5 mM NaF, 1 mM PMSF, 1 µL/mL protease inhibitor cocktail (Sigma) and clarified by centrifugation at 1600g for 5 min at 4°C. To evaluate RhoA activity, 300 µg of the protein lysates were incubated with 50 ug of Rhotekin-RBD beads (Cytoskeleton), for 1 hour at 4°C for RhoA, or with 100 mg of GST-fusion protein, containing CRIB domain of PAK (GST–PAK), attached to beads (Sigma) for Rac1. Beads pellet were washed two times with 25 mM Tris pH 7.5, 0.5% NP40, 40 mM NaCl, 30 mM MgCl2, 1 mM DTT, 1mM PMSF, 1 uL/mL protease inhibitor cocktail (Sigma) before addition of 5X Laemmli buffer.

Fractions were analysed by western blotting. Proteins were separated on a 12% SDS polyacrylamide gel and transfered onto a PVDF membrane (GE Healthcare) for RhoA and onto a nitrocellulose membrane for Rac1. Blots were probed with either mouse monoclonal anti-RhoA (1:200, Santa Cruz) or anti-Rac1 (1:1000, Transduction Laboratories).

The band density was quantified by Fusion software (Vilber Lourmat). The relative densities of pulled down RhoA were normalized to the total RhoA, in the same sample.

Averages were analysed and standard deviations (SD) were calculated. Differences were considered as significant when $P<0.05$ using Student's *t* test.

Axonal tracing

After intracardiac perfusion with 4% PFA in 0.12M phosphate buffer, pH 7.4, embryonic dissected brains were fixed at least overnight at 4°C in 4% PFA. Small crystals of DiI (1,1'-dioctadecyl 3,3,3',3'-tetramethylindocarbocyanine perchlorate ; D282, Molecular probes, Eugene, OR) and/or DiA (4-4-dihexadecyl aminostryryl N-methyl-pyridinium iodide ; D291, Molecular probe, Eugene, OR) were inserted into the thalamus of E16.5 (for anterograde tracings) or the neocortex of E18.5 (for retrograde tracings) after hemi-dissection of the brains, and let diffuse at 37°C (from one to three weeks in the dark). The status of the dye diffusion was assessed by whole-brain examination under the fluorescent binocular set-up (Leica MZ16F).

Subsequently, brains were embedded in 3% agarose and cut at a thickness of 80 µm with a vibratome. Hoechst (sigma) was used for fluorescent nuclear conterstaining. The sections were mounted in PBS, observed, and photographed by using appropriate filters.

Cell lines stimulation by Slit-2

After serum starvation and before use, primary MEFs were cultured in the presence of 3 DIV conditioned medium from EBNA 293 secreting *Xenopus* slit (EBNA-slit; (Wu et al., 1999); (Chen et al., 2000) fused in frame at its C terminus to a myc tag (Li et al., 1999). the *Xenopus slit* is an orthologue of the mouse and human *slit-2* genes (Li et al., 1999). The efficiency of the commercially available mouse Slit2 and of conditioned medium from cells stably secreting xSlit was equivalent. Note that MEFs cells from control and *trio-/-* embryos express Robo1 and Robo2 endogenously as illustrated on Fig. S1A, and that Trio is totally absent in *trio-/-* MEFs (Fig. S1A).

Immunoprecipitation and Western blot

Lysates were prepared from MEFs. Cells were washed with cold PBS and lysed in buffer containing 25 mM Tris-HCL pH 7.5, 100 mM NaCl, 1 mM EDTA, 1 mM DTT, 1mM PMSF, 2% Triton, for 15 min on ice and centrifugated at 16,000 *g* for 30 min at 4°C. Proteins were boiled with the Laemmli loading buffer, resolved on a 6% polyacrylamide gel and blotted on to nitrocellulose membrane (Amersham, UK). After saturation in TBST with 5% milk, membranes were incubated with the

following primary antibodies: anti-Robo1 (a kind gift from F. Murakami, Osaka, Japan), anti-Robo2 (a kind gift from F. Murakami, Osaka, Japan; (Andrews et al., 2006), anti-Trio (clone H120, Santa Cruz Laboratories). Primary antibodies were revealed by incubation with HRP-conjugated anti-mouse or anti-rabbit IgG (1:25,000; Santa Cruz Laboratories). Bands were revealed with Femto ECL (Pierce ThermoFisher).

Statistical analysis

Quantitative data sets were analysed using a two-way ANOVA with Bonferroni's multiple comparison test (Fig. 1A) using GraphPad Prism 6 software, and a student t-test (Fig. 1B). For quantifications of collapse assays (Fig. 6M), a Fisher's exact test was performed using GraphPad Prism software to determine whether the qualitative variables (collapsed and non-collapsed growth cones / with or without Slit2 stimulation) were independent. Statistical significance were set at a p value < 0.05 (*), $p<0.01$ (**) and $p<0.0001$ (****), non significant (ns): $p>0.05$.

AUTHOR CONTRIBUTIONS

S.B. was the primary experimentalist and contributed to the whole experimental work. L.L. supported S.B, brought decisive experiments, proposed and contributed to the axonal tracing experimental work, and to the collapse analyses experiments. C.L. worked under SB's supervision. M.D. participated in the initiation of experiments and collaboration. S.G. participated in the scientific elaboration and analyses of the study. E.B-G conceived the study design, directed experiments, performed some experiments and wrote the manuscript. All the authors edited the manuscript.

ACKNOWLEDGEMENTS

We thank Christine Métin, Serge Marty, Valérie Doye and Jérôme Delon for their helpful suggestions and critical reading of the manuscript. We also thank Luis Puelles for his advice in neuro-anatomy. We would like to thank Annie Goldman for English proofreading and INSERM and FRM (Contract N°DCM20111223066) for their financial support.

COMPETING INTERESTS

The authors declare that they have no conflict of interest

REFERENCES

Andrews, W., Liapi, A., Plachez, C., Camurri, L., Zhang, J., Mori, S., Murakami, F., Parnavelas, J. G., Sundaresan, V. and Richards, L. J. (2006). Robo1 regulates the development of major axon tracts and interneuron migration in the forebrain. *Development* **133**, 2243-2252.

Ba, W., Yan, Y., Reijnders, M. R., Schuurs-Hoeijmakers, J. H., Feenstra, I., Bongers, E. M., Bosch, D. G., De Leeuw, N., Pfundt, R., Gilissen, C., et al. (2016). TRIO loss of function is associated with mild intellectual disability and affects dendritic branching and synapse function. *Human molecular genetics* **25**, 892-902.

Backer, S., Hidalgo-Sanchez, M., Offner, N., Portales-Casamar, E., Debant, A., Fort, P., Gauthier-Rouviere, C. and Bloch-Gallego, E. (2007). Trio controls the mature organization of neuronal clusters in the hindbrain. *J Neurosci* **27**, 10323-10332.

Bellanger, J. M., Lazaro, J. B., Diriong, S., Fernandez, A., Lamb, N. and Debant, A. (1998). The two guanine nucleotide exchange factor domains of Trio link the Rac1 and the RhoA pathways in vivo. *Oncogene* **16**, 147-152.

Bielle, F., Marcos-Mondejar, P., Keita, M., Mailhes, C., Verney, C., Nguyen Ba-Charvet, K., Tessier-Lavigne, M., Lopez-Bendito, G. and Garel, S. (2011). Slit2 activity in the migration of guidepost neurons shapes thalamic projections during development and evolution. *Neuron* **69**, 1085-1098.

Blangy, A., Vignal, E., Schmidt, S., Debant, A., Gauthier-Rouviere, C. and Fort, P. (2000). TrioGEF1 controls Rac- and Cdc42-dependent cell structures through the direct activation of rhoG. *J Cell Sci* **113 (Pt 4)**, 729-739.

Bloch-Gallego, E., Ezan, F., Tessier-Lavigne, M. and Sotelo, C. (1999). Floor plate and netrin-1 are involved in the migration and survival of inferior olivary neurons. *J Neurosci* **19**, 4407-4420.

Braisted, J. E., Catalano, S. M., Stimac, R., Kennedy, T. E., Tessier-Lavigne, M., Shatz, C. J. and O'Leary, D. D. (2000). Netrin-1 promotes thalamic axon growth and is required for proper development of the thalamocortical projection. *The Journal of neuroscience : the official journal of the Society for Neuroscience* **20**, 5792-5801.

Briancon-Marjollet, A., Ghogha, A., Nawabi, H., Triki, I., Auziol, C., Fromont, S., Piche, C., Enslen, H., Chebli, K., Cloutier, J. F., et al. (2008). Trio mediates netrin-1-induced Rac1 activation in axon outgrowth and guidance. *Molecular and cellular biology* **28**, 2314-2323.

Castellani, V., Chedotal, A., Schachner, M., Faivre-Sarrailh, C. and Rougon, G. (2000). Analysis of the L1-deficient mouse phenotype reveals cross-talk between Sema3A and L1 signaling pathways in axonal guidance. *Neuron* **27**, 237-249.

Castillo-Paterna, M., Moreno-Juan, V., Filipchuk, A., Rodriguez-Malmierca, L., Susin, R. and Lopez-Bendito, G. (2015). DCC functions as an accelerator of thalamocortical axonal growth downstream of spontaneous thalamic activity. *EMBO Rep* **16**, 851-862.

Causeret, F., Hidalgo-Sanchez, M., Fort, P., Backer, S., Popoff, M. R., Gauthier-Rouviere, C. and Bloch-Gallego, E. (2004). Distinct roles of Rac1/Cdc42 and Rho/Rock for axon outgrowth and nucleokinesis of precerebellar neurons toward netrin 1. *Development* **131**, 2841-2852.

Chen, J. H., Wu, W., Li, H. S., Fagaly, T., Zhou, L., Wu, J. Y. and Rao, Y. (2000). Embryonic expression and extracellular secretion of Xenopus slit. *Neuroscience* **96**, 231-236.

Cherfils, J. and Zeghouf, M. (2013). Regulation of small GTPases by GEFs, GAPs, and GDIs. *Physiol Rev* **93**, 269-309.

Debant, A., Serra-Pages, C., Seipel, K., O'Brien, S., Tang, M., Park, S. H. and Streuli, M. (1996). The multidomain protein Trio binds the LAR transmembrane tyrosine phosphatase, contains a protein kinase domain, and has separate rac-specific and rho-specific guanine nucleotide exchange factor domains. *Proc Natl Acad Sci U S A* **93**, 5466-5471.

Deck, M., Lokmane, L., Chauvet, S., Mailhes, C., Keita, M., Niquille, M., Yoshida, M., Yoshida, Y., Lebrand, C., Mann, F., et al. (2013). Pathfinding of corticothalamic axons relies on a rendezvous with thalamic projections. *Neuron* **77**, 472-484.

DeGeer, J., Boudeau, J., Schmidt, S., Bedford, F., Lamarche-Vane, N. and Debant, A. (2013). Tyrosine phosphorylation of the Rho guanine nucleotide exchange factor Trio regulates netrin-1/DCC-mediated cortical axon outgrowth. *Molecular and cellular biology* **33**, 739-751.

DeGeer, J., Kaplan, A., Mattar, P., Morabito, M., Stochaj, U., Kennedy, T. E., Debant, A., Cayouette, M., Fournier, A. E. and Lamarche-Vane, N. (2015). Hsc70 chaperone activity underlies Trio GEF function in axon growth and guidance induced by netrin-1. *The Journal of cell biology* **210**, 817-832.

Di Donato, N., Jean, Y. Y., Maga, A. M., Krewson, B. D., Shupp, A. B., Avrutsky, M. I., Roy, A., Collins, S., Olds, C., Willert, R. A., et al. (2016). Mutations in CRADD Result in Reduced Caspase-2-Mediated Neuronal Apoptosis and Cause Megalencephaly with a Rare Lissencephaly Variant. *American journal of human genetics* **99**, 1117-1129.

Fouquet, C., Di Meglio, T., Ma, L., Kawasaki, T., Long, H., Hirata, T., Tessier-Lavigne, M., Chedotal, A. and Nguyen-Ba-Charvet, K. T. (2007). Robo1 and robo2 control the development of the lateral olfactory tract. *The Journal of neuroscience : the official journal of the Society for Neuroscience* **27**, 3037-3045.

Jaffe, A. B. and Hall, A. (2005). Rho GTPases: biochemistry and biology. *Annu Rev Cell Dev Biol* **21**, 247-269.

Katrancha, S. M., Wu, Y., Zhu, M., Eipper, B. A., Koleske, A. J. and Mains, R. E. (2017). Neurodevelopmental disease-associated de novo mutations and rare sequence variants affect TRIO GDP/GTP exchange factor activity. *Hum Mol Genet* **26**, 4728-4740.

Lawson, C. D. and Burridge, K. (2014). The on-off relationship of Rho and Rac during integrin-mediated adhesion and cell migration. *Small GTPases* **5**, e27958.

Li, H. S., Chen, J. H., Wu, W., Fagaly, T., Zhou, L., Yuan, W., Dupuis, S., Jiang, Z. H., Nash, W., Gick, C., et al. (1999). Vertebrate slit, a secreted ligand for the transmembrane protein roundabout, is a repellent for olfactory bulb axons. *Cell* **96**, 807-818.

Liu, X., Lu, Y., Zhang, Y., Li, Y., Zhou, J., Yuan, Y., Gao, X., Su, Z. and He, C. (2012). Slit2 regulates the dispersal of oligodendrocyte precursor cells via Fyn/RhoA signaling. *The Journal of biological chemistry* **287**, 17503-17516.

Lokmane, L. and Garel, S. (2014). Map transfer from the thalamus to the neocortex: inputs from the barrel field. *Semin Cell Dev Biol* **35**, 147-155.

Lokmane, L., Proville, R., Narboux-Neme, N., Gyory, I., Keita, M., Mailhes, C., Lena, C., Gaspar, P., Grosschedl, R. and Garel, S. (2013). Sensory map transfer to the neocortex relies on pretarget ordering of thalamic axons. *Curr Biol* **23**, 810-816.

Long, H., Yoshikawa, S. and Thomas, J. B. (2016). Equivalent Activities of Repulsive Axon Guidance Receptors. *The Journal of neuroscience : the official journal of the Society for Neuroscience* **36**, 1140-1150.

Lopez-Bendito, G., Cautinat, A., Sanchez, J. A., Bielle, F., Flames, N., Garratt, A. N., Talmage, D. A., Role, L. W., Charnay, P., Marin, O., et al. (2006). Tangential neuronal migration controls axon guidance: a role for neuregulin-1 in thalamocortical axon navigation. *Cell* **125**, 127-142.

McMullan, R., Anderson, A. and Nurrish, S. (2012). Behavioral and immune responses to infection require Galphaq- RhoA signaling in C. elegans. *PLoS Pathog* **8**, e1002530.

Nakamura, F. (2013). FilGAP and its close relatives: a mediator of Rho-Rac antagonism that regulates cell morphology and migration. *The Biochemical journal* **453**, 17-25.

Nguyen-Ba-Charvet, K. T., Plump, A. S., Tessier-Lavigne, M. and Chedotal, A. (2002). Slit1 and slit2 proteins control the development of the lateral olfactory tract. *The Journal of neuroscience : the official journal of the Society for Neuroscience* **22**, 5473-5480.

O'Brien, S. P., Seipel, K., Medley, Q. G., Bronson, R., Segal, R. and Streuli, M. (2000). Skeletal muscle deformity and neuronal disorder in Trio exchange factor-deficient mouse embryos. *Proc Natl Acad Sci U S A* **97**, 12074-12078.

Plageman, T. F., Jr., Chauhan, B. K., Yang, C., Jaudon, F., Shang, X., Zheng, Y., Lou, M., Debant, A., Hildebrand, J. D. and Lang, R. A. (2011). A Trio-RhoA-Shroom3 pathway is required for apical constriction and epithelial invagination. *Development* **138**, 5177-5188.

Portales-Casamar, E., Briancon-Marjollet, A., Fromont, S., Triboulet, R. and Debant, A. (2006). Identification of novel neuronal isoforms of the Rho-GEF Trio. *Biol Cell* **98**, 183-193.

Powell, A. W., Sassa, T., Wu, Y., Tessier-Lavigne, M. and Polleux, F. (2008). Topography of thalamic projections requires attractive and repulsive functions of Netrin-1 in the ventral telencephalon. *PLoS Biol* **6**, e116.

Sadybekov, A., Tian, C., Arnesano, C., Katritch, V. and Herring, B. E. (2017). An autism spectrum disorder-related de novo mutation hotspot discovered in the GEF1 domain of Trio. *Nat Commun* **8**, 601.

Schmidt, S. and Debant, A. (2014). Function and regulation of the Rho guanine nucleotide exchange factor Trio. *Small GTPases* **5**, e29769.

Settleman, J. (2003). A nuclear MAL-function links Rho to SRF. *Mol Cell* **11**, 1121-1123.

Tcherkezian, J. and Lamarche-Vane, N. (2007). Current knowledge of the large RhoGAP family of proteins. *Biol Cell* **99**, 67-86.

Wong, K., Ren, X. R., Huang, Y. Z., Xie, Y., Liu, G., Saito, H., Tang, H., Wen, L., Brady-Kalnay, S. M., Mei, L., et al. (2001). Signal transduction in neuronal migration: roles of GTPase activating proteins and the small GTPase Cdc42 in the Slit-Robo pathway. *Cell* **107**, 209-221.

Wu, W., Wong, K., Chen, J., Jiang, Z., Dupuis, S., Wu, J. Y. and Rao, Y. (1999). Directional guidance of neuronal migration in the olfactory system by the protein Slit. *Nature* **400**, 331-336.

Figures

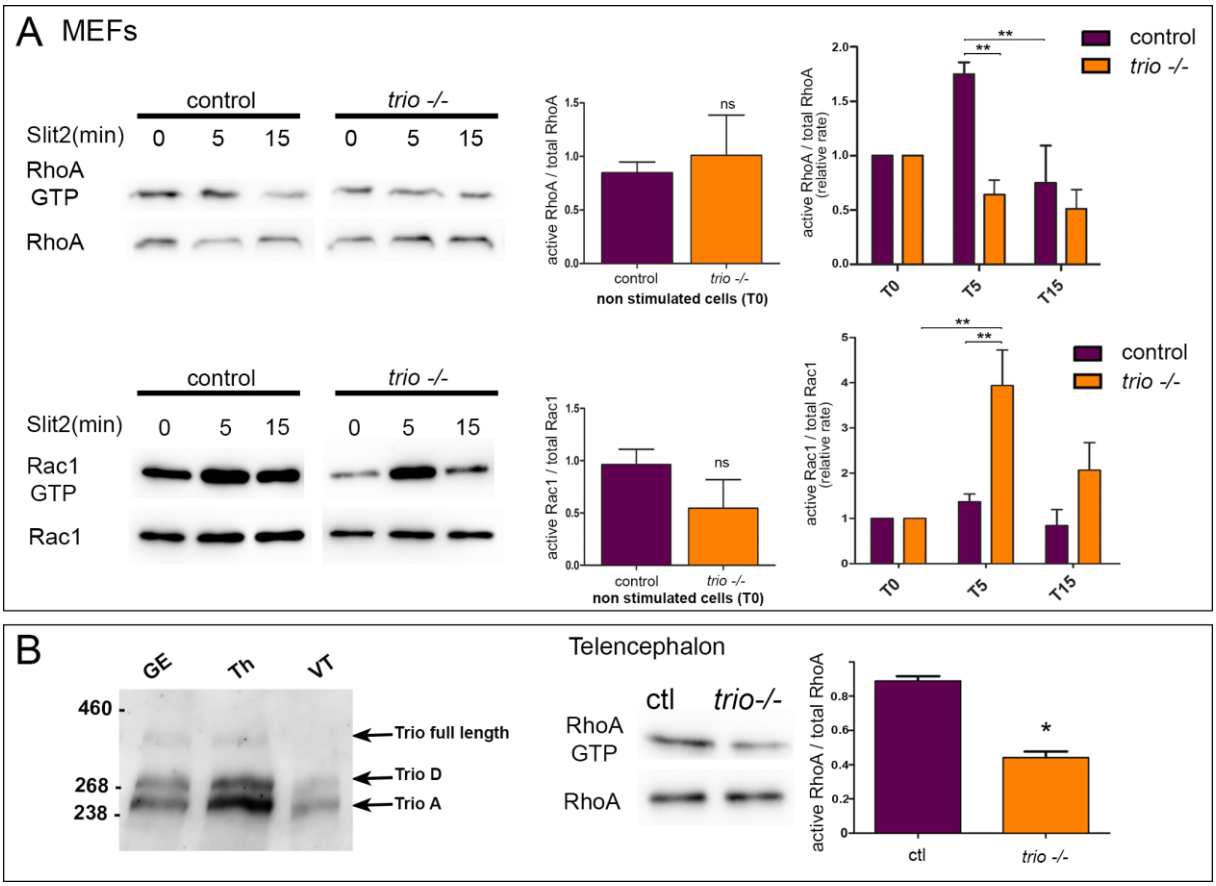

Figure 1: Trio is required to mediate RhoA activation upon Slit2 stimulation.

(A) **Upon Slit2 stimulation, RhoA activation depends on the expression of Trio whereas Rac1 activation occurs only in the absence of Trio.**

MEFs obtained from either control wild type animals (control, n=4) or from *trio*$^{-/-}$ mutant mice (n=4) were - or not - stimulated for different periods of time with Slit2. RhoA activity was then measured to evaluate the relative rate of active and total RhoA protein in the corresponding cell extracts. Western blots from control or mutant MEFs cultures were probed with RhoA antisera after pull-down assays using GST-Rhotekin. Quantification from 4 experiments expressed the ratio of activated RhoA GTPase signal normalized to total RhoA in protein extracts from MEFs. Similar assays have been conducted for Slit-2 stimulation on MEFs from control wild type animals (control, n=3) or from *trio*$^{-/-}$ mutant mice (n=3), and revealed for Rac1 activation. Western blots from control or mutant MEFs cultures were probed with Rac1 antibody after pull-down assays using GST-PAK. Quantification from

4 experiments expressed as the ratio of activated Rac1 GTPase signal normalized to total Rac1 in protein extracts from MEFs. Upon a 5-minute Slit2 stimulation, the activity of RhoA is increased but is strictly dependent on the presence of Trio. On the contrary, Rac1 activation in MEFs is significantly increased after a 5-minute Slit2 stimulation, exclusively in the absence of Trio.

The activation states are compared between paired MEFs samples from control and *trio*$^{-/-}$ animals of the same littermate and statistically analysed using a two-way ANOVA with Bonferroni's multiple comparison test. p values were noted ** for $p<0.001$, * for $p<0.05$ and ns for non significant ($p>0.05$).

(B) **RhoA activation is impaired in the absence of Trio *in vivo*.**

The full length Trio (350 kDa) is slightly detected in ventral telencephalon (VT) extracts. Trio is mainly expressed as spliced isoforms migrating as a doublet - slightly above the 250kDa MW marker band - which is likely to correspond to Trio D (300kDa) and Trio A (250kDa), as well as in ganglionc eminences (GE) and thalamus (Th) extracts.

Quantification of the relative active state of RhoA as in (C), after pull-down assays using GST-Rhotekin and ventral telencephalon extracts from E14 wild type (n=3) mice and *trio*$^{-/-}$ mice (n=3) and Western blot. The activation states are compared between paired control and mutant animals obtained from the same littermates. Four different littermates have been used for this experiment. Bars illustrate SEM. The Student's *t* test established p=0,019 (*).

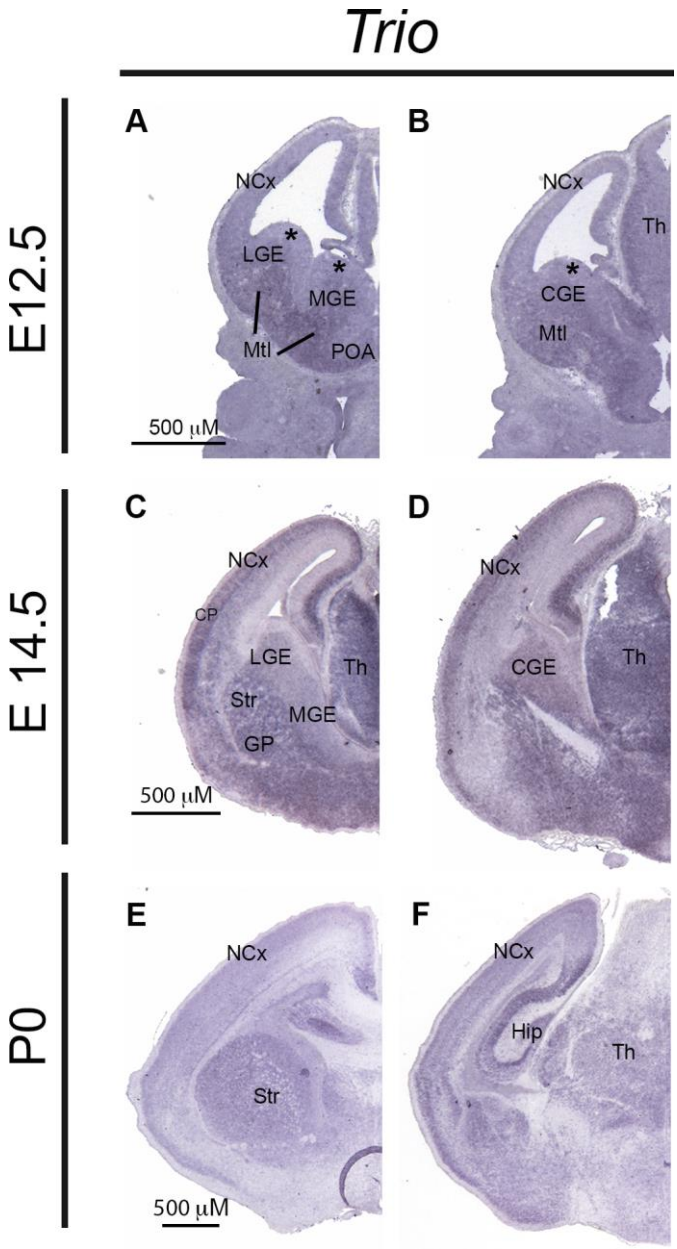

Figure 2: Expression of *Trio* transcripts in mouse telencephalon and thalamus at embryonic day 12.5, 14.5 and at birth.

At E12.5 (A, B), *Trio* expression is located in the mantle layer (Mtl) of both LGE and MGE while it is absent in the ventricular and subventricular zones of both (asterisks in A, B)

At E14.5 (C, D), *Trio* is strongly expressed in the thalamus (Th) and in the ventral part of the telencephalon, including the striatum (Str), and the mantle of MGE, LGE and CGE. A strong *Trio* expression is also observed in the subcortical plate of the neocortex (NCx). At birth (P0; E F), *Trio* transcripts are present among other regions, in the striatum and thalamus. (Scale bar: 500 µm).

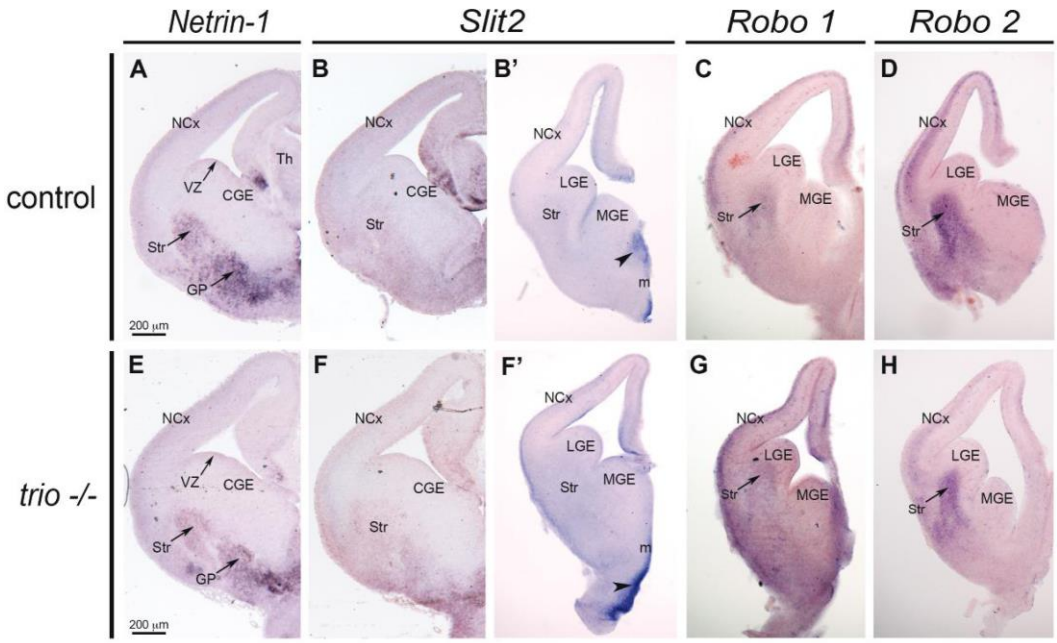

Figure 3: Expression domains of Netrin-1, Slit2, Robo1 and Robo2 transcripts in E14.5 control and *trio*$^{-/-}$ embryos.

Coronal sections through mid-telencephalic/rostral diencephalic levels of E14.5 control and *trio*$^{-/-}$ embryos have been used to analyse the expression of Netrin-1 (A, E) and Slit2 (B, B', F, F') mRNAs using cryosections, and the one of Robo1 (C, G) and Robo2 (D-H) using vibratome sections. At E14.5, in the absence of TRIO (E), the ventricular zone of the LGE, the whole striatum in the mantle zone and the most dorsal part of the thalamus still express *Netrin-1* transcripts as in control animals (compare A, control and E, *trio*$^{-/-}$). Slit2 transcripts are visualized after ISH in control (B, B') and *trio*$^{-/-}$ (F, F') embryos: the ventral midline (m) and the ventricular zones of the lateral and medial ganglionic eminences (LGE, MGE; B', F') express Slit mRNAs. *Robo1* (C, G) and *Robo2* (D, H) transcripts remain expressed in identical areas in both control (C, D) and *trio*$^{-/-}$ (G, H) E14.5 embryos. In both control and mutant embryos, *Robo 1* and *Robo2* transcripts are expressed in the neocortex (NCx; C, D) and dorsal thalamus (non illustrated) in a partially complementary manner. Robo1 and Robo2 transcripts are expressed in the mantle, but with a higher expression level for Robo2. Str, striatum; MGE, medial ganglionic eminence; LGE, lateral ganglionic eminence. Scale bars: A-H, 200 µm

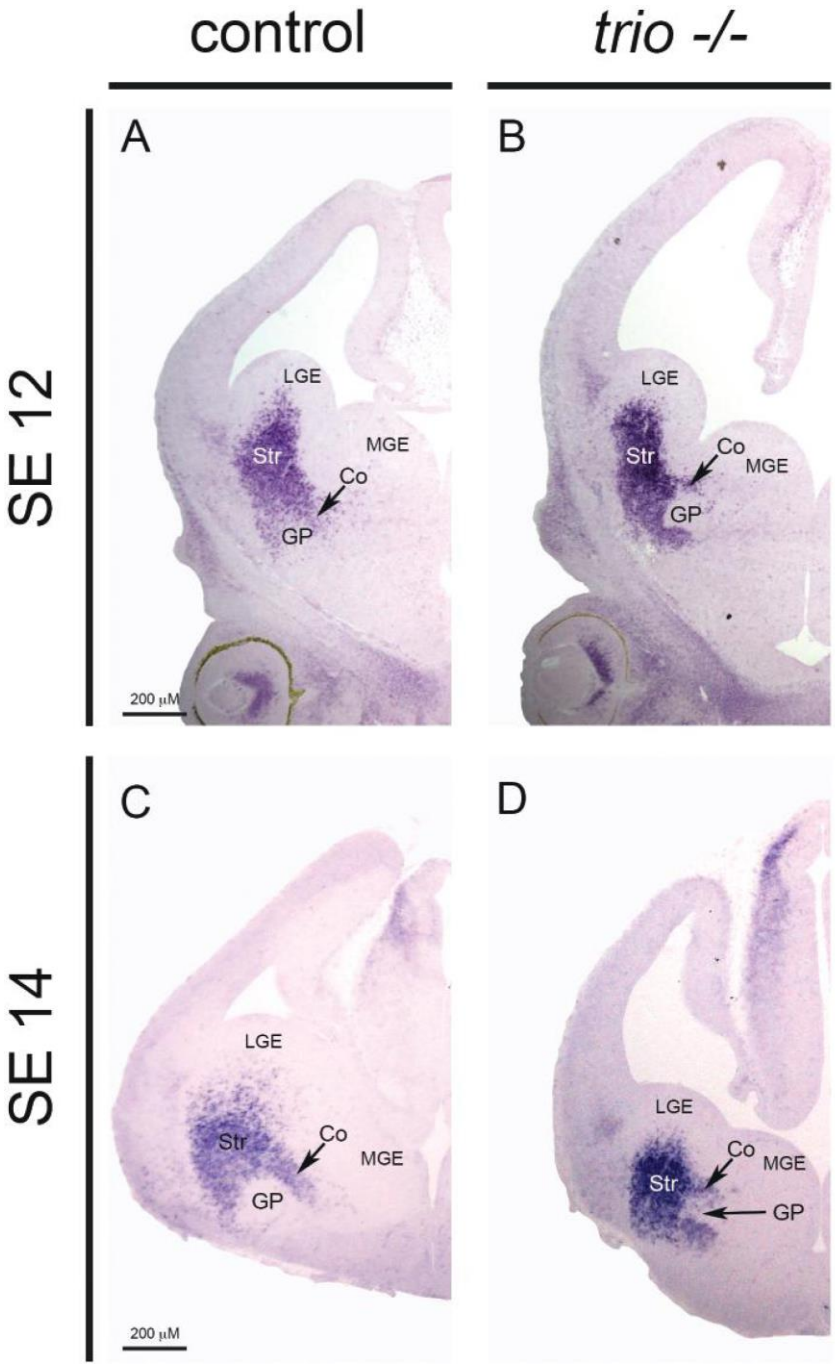

Figure 4: Guidepost cells fail to position properly from the LGE to the MGE to set up the corridor in *trio*$^{-/-}$ *mice.*

Both corridor cells (Co) and striatum (Str) have been visualized through their *Ebf1* expression. The shape of the corridor cells migratory path is abnormal in *trio*$^{-/-}$, both at E12.5 (n=2 for both mutant and control, compare B and A) and at E14.5 (n=5, for both mutant and control, compare D and C). The migratory path is compacted, shortened in the absence of Trio, and misoriented (Scale bar: 200µm).

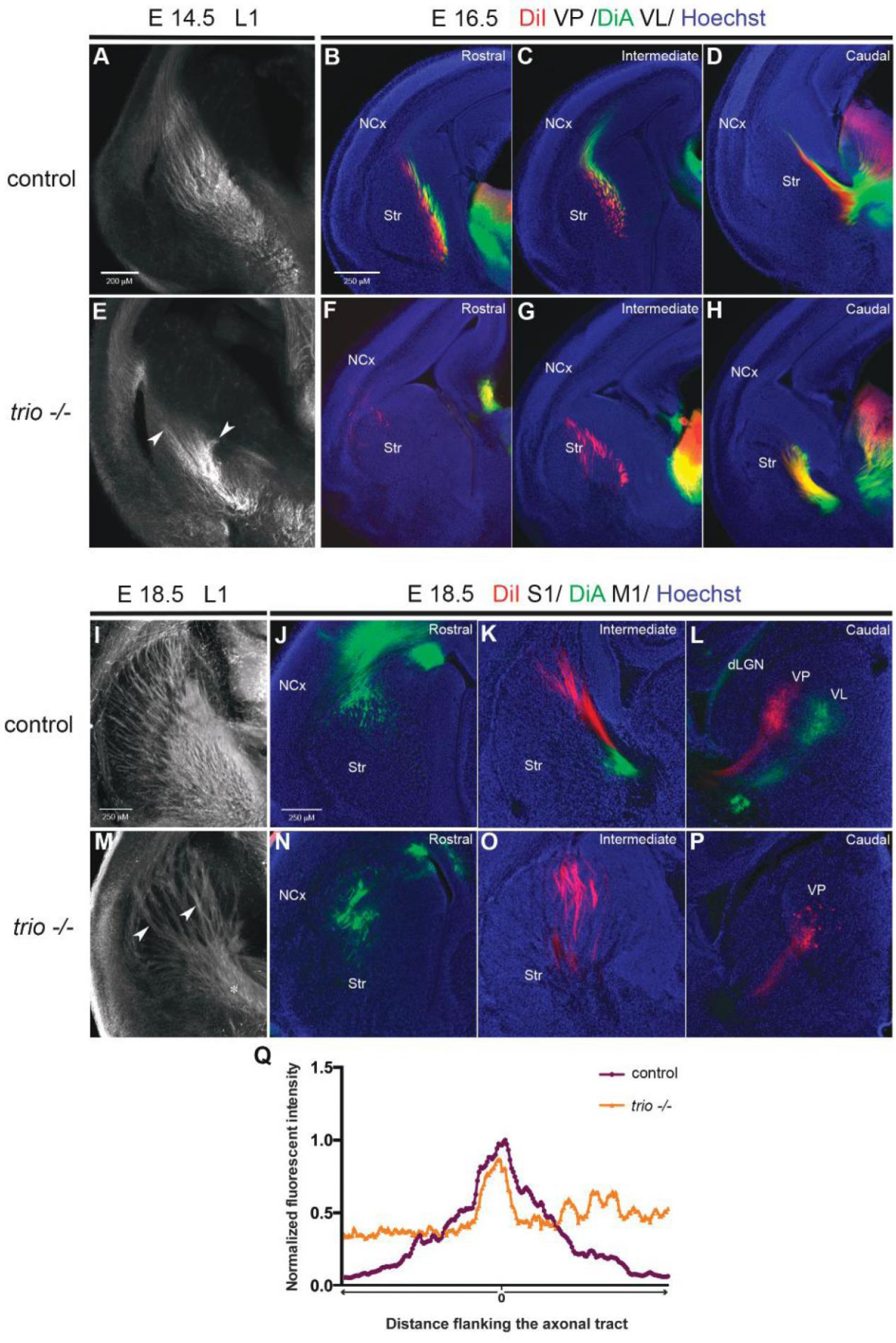

Figure 5: Analysis of the pathfinding of thalamocortical axons (TCA) in both control and *trio*$^{-/-}$ embryos by L1 immunostaining and axonal tracings.

We have analysed the trajectories of TCA using L1 immunostaining at E14.5 (A, E) and E18.5 (I, M). In *trio*$^{-/-}$ mutants, axons are compacted, forming bundles across the striatum, contrary to their spread aspect in the control when invading the whole striatum with a fan shape. At E14.5, L1 immunolabeling reveals a ventral confinement of TCA in *trio* mutant mice (E, n=5). They are delayed instead of turning and reorienting rostrally across the striatum as observed in control mice at this stage (A, n=5). Thus the striatum is abnormally shaped and perforated by TCA bundles at E14.5 and E18.5 (n=3) in the absence of Trio. DiI was injected in the ventro-posterior nucleus of the thalamus (VP) and DiA in the ventro-lateral thalamus (VL) at E16.5. The resulting anterograde tracing to the cortex has been analysed on vibratome sections. It is noteworthy to underline that in E16.5 (B-D, n=3) wild type forebrains, TCA cross the subpallium forming a compact internal capsule with TCA growing in the striatum (Str), and show a linear organisation of axon fascicles to reach the cortical subplate, whereas the axonal trajectory is severely affected in *trio*$^{-/-}$ and few of them reach the neocortex (F-H, n=3). Axonal labelling is also analysed at different levels of the brain (rostral, intermediate and caudal) after injection of carbocyanines crystals in the E18.5 neocortex (NCx) DiA in the motor neocortex and DiI in the somatosensory neocortex. In wild type (J-L, n=5), motor and somatosensory axons follow a stereotyped trajectory through the subpallium. Retrograde tracing at E18.5 also allows the anterograde labelling of the reciprocal corticothalamic axons (CTA). In *trio-/-* (N-P, n=3), DiA injection at a rostral level shows that CTA grow out of the neocortex and invade the striatum but stop, while DiI injection reveals the disorganized trajectory through the subpallium as well as a retrolabelling in the thalamus indicating that TCA can reach the neocortex. (Scale bar: 200µm). The quantification of the dispersion of the thalamic tractus at E18.5 using ImageJ is illustrated in Q.

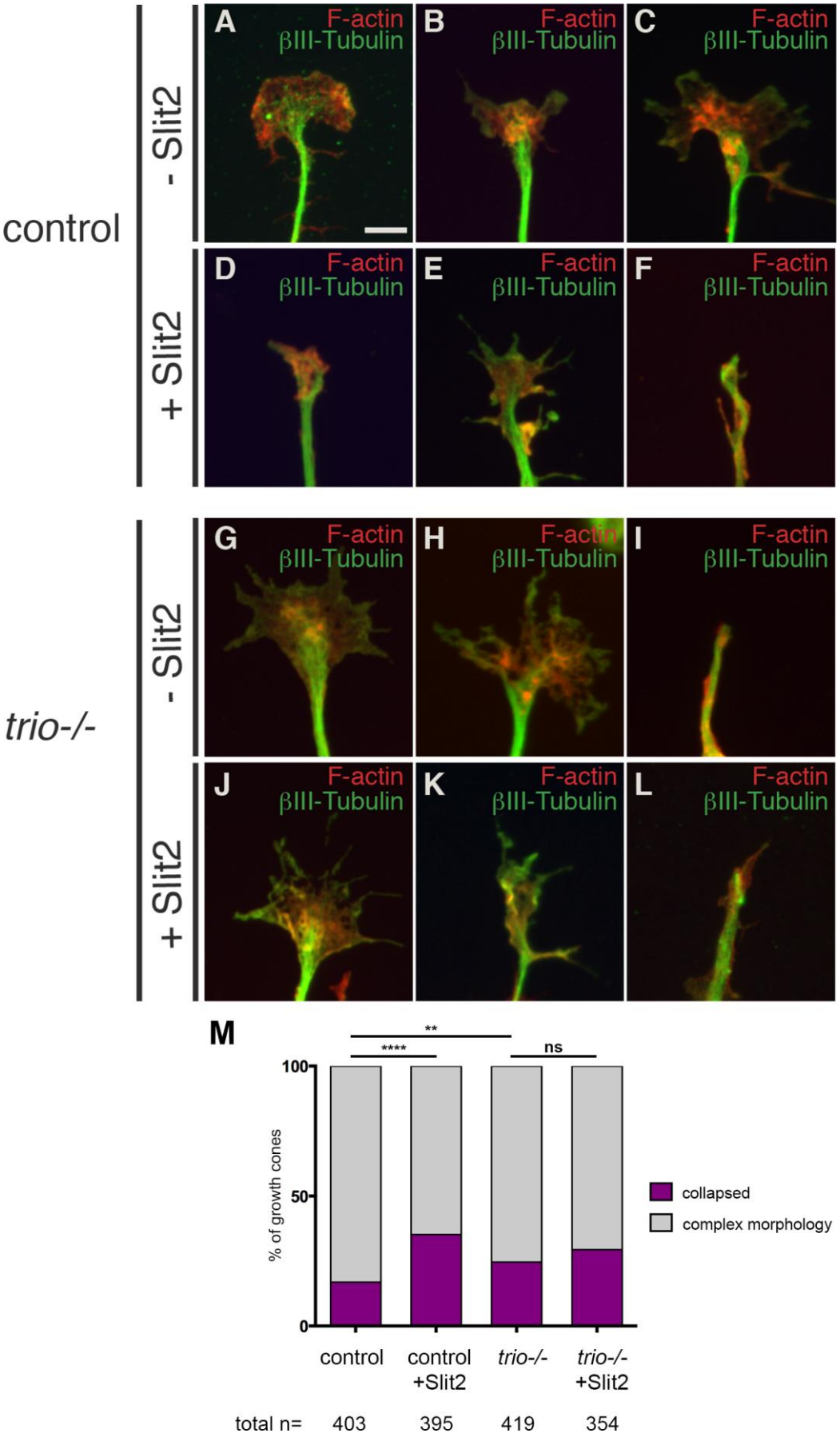

Figure 6: Slit2-induced collapse of thalamic growth cones depends on the presence of Trio.

(A-L) Collapse assays on E13.5 dissociated thalamic neurons from wild type (A-F) or *trio*$^{-/-}$ embryos (G-L) in the presence (D-F and J-L) or absence (A-C and G-I) of Slit2. Phalloidin and Tuj1 double staining allows the visualization of the complex morphologies of growth cones or their collapsed aspect (as observed in F, I, L). Scale bars, 5 μm.

(M) Quantifications of collapse were performed with 5 wild type and 6 *trio*$^{-/-}$ mutants from 3 distinct littermates. For each condition, the total number of growth cones analyzed is indicated (n=).

Note that unlike in wild type neurons, the percentage of axonal growth cones collapsing is not significantly increased in response to Slit2 in *trio*$^{-/-}$ thalamic neurons. ns: $P>0.05$; **** $P< 0.0001$ and ** $P< 0.008$ using a Fisher exact probability test.

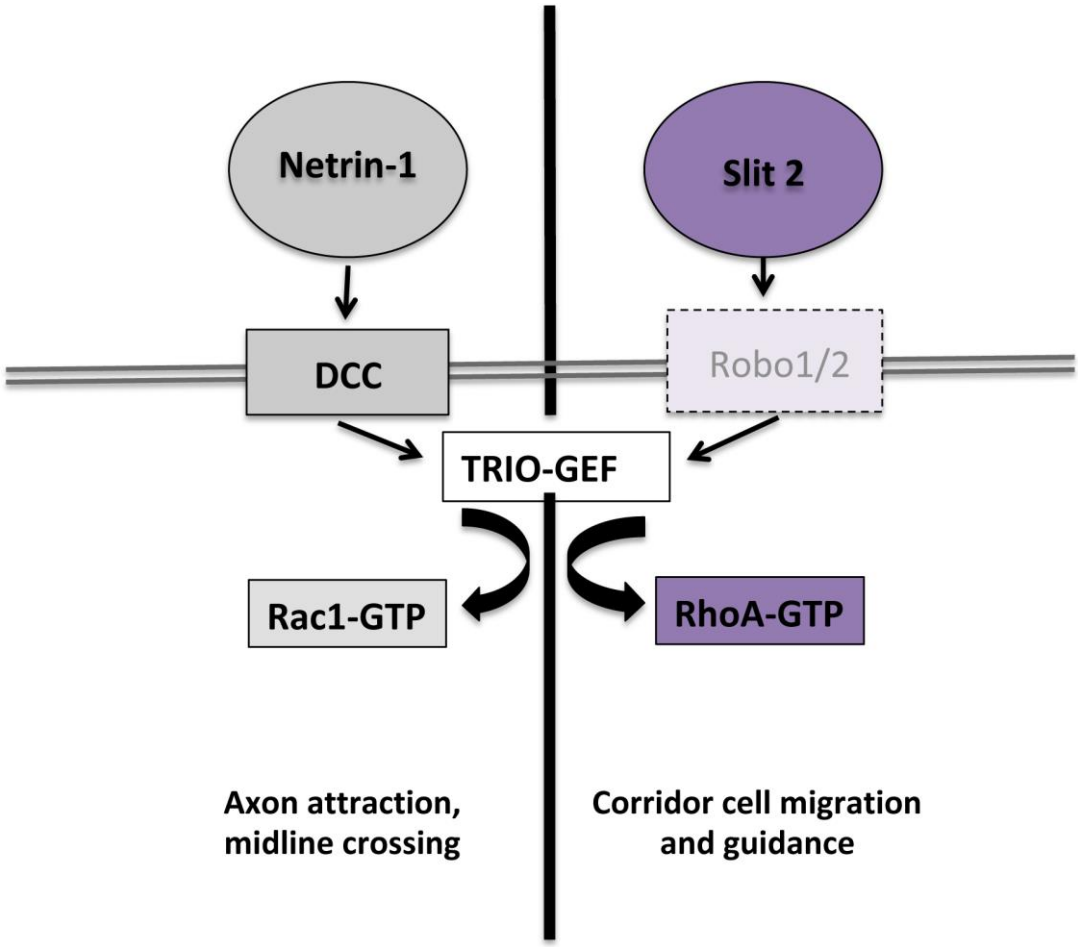

Figure 7: Trio as a possible bottleneck: a model of the integrative signalling pathway.

Trio-GEF carries two GEF domains. The GEF1 domain has already been shown to be activated downstream Netrin-1 binding on DCC receptors in mammals, and it allows axon attraction and this pathway also allows axon crossing the midline. The present data demonstrate that Slit2 is able to stimulate RhoA activation during mouse telencephalon embryonic development. Thus Trio acts a master-integrator for Slit/RhoA signalling through a Trio RhoA GEF activity, in addition to Netrin-1/DCC/Rac1 activation through its Trio Rac1 GEF activity. Whether Slit/RhoA pathway involves exclusively or not Robo receptors – that are expressed in the telencephalic regions (Fig. 3 and Fig. S1B) – remains to be determined. Therefore Trio is a bottleneck for transducing guidance cues and cytoskeleton remodeling in the processes of both axon outgrowth/pathfinding and neuronal migration during embryonic development of the rostral CNS. The signaling pathway that allows RhoA activation downstream Trio-GEF is functional *in vivo* and it allows the proper migration and positioning of corridor cells.

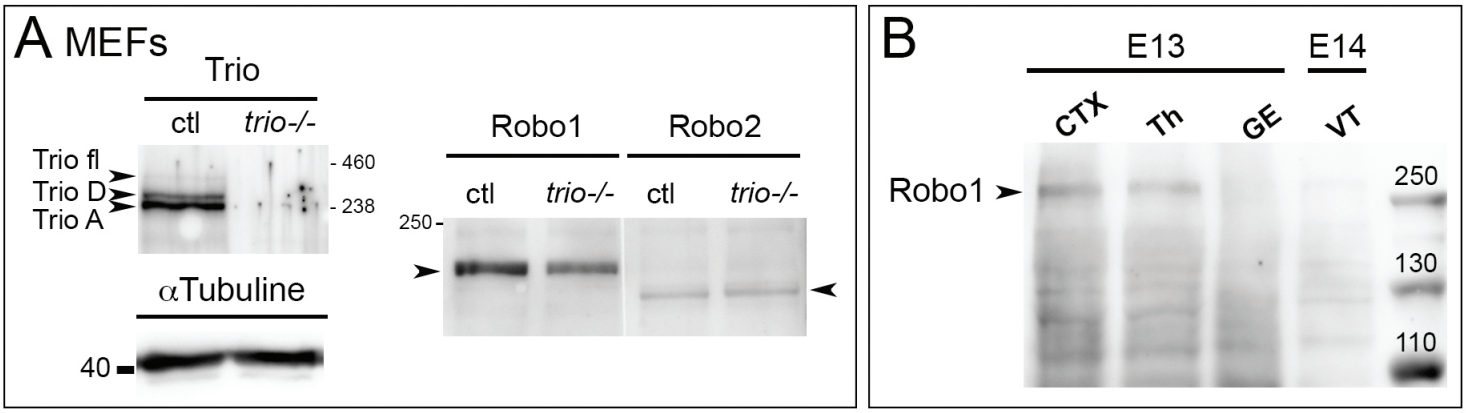

Supplemental Figure 1 (Figure S1)

(A) Trio is absent in trio-/-, while Robo1/2 receptors are properly expressed.
Extracts from MEFs from either control or trio-/- mice have been used to visualize upon Western blot
the amount of remaining Trio, and the expression of Robo1/2. Both sources of MEFs expressed comparable levels of endogenously Robo1/2 receptors but MEFs isolated from the Trio KO did not express Trio anymore. The expression level of α-Tubulin, used as an internal control, remains unchanged.

(B) Robo1 is expressed in telencephalic and thalamic extracts.
Extracts from cortex (CTX), thalamus (Th) and ganglionic eminences (GE) at E13 and ventral telencephalon extract at E14 have been used to visualize Robo1 expression by
Western blot. Its higher expression is visualized in E13 cortical and thalamic extract.

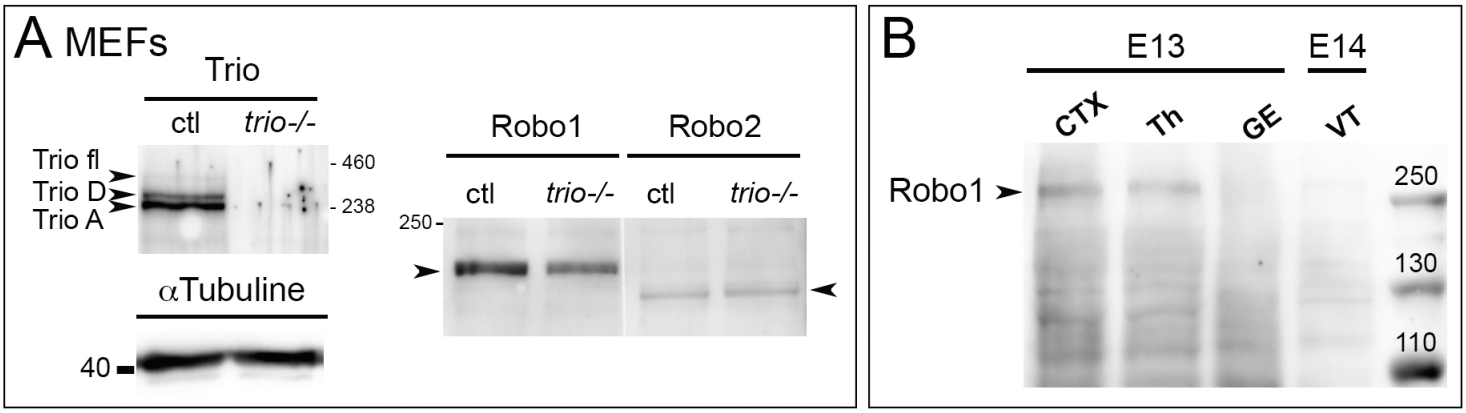

Supplemental Figure 1 (Figure S1)

(A) Trio is absent in trio-/-, while Robo1/2 receptors are properly expressed.
Extracts from MEFs from either control or trio-/- mice have been used to visualize upon Western blot
the amount of remaining Trio, and the expression of Robo1/2. Both sources of MEFs expressed comparable levels of endogenously Robo1/2 receptors but MEFs isolated from the Trio KO did not express Trio anymore. The expression level of α-Tubulin, used as an internal control, remains unchanged.

(B) Robo1 is expressed in telencephalic and thalamic extracts.
Extracts from cortex (CTX), thalamus (Th) and ganglionic eminences (GE) at E13 and ventral telencephalon extract at E14 have been used to visualize Robo1 expression by
Western blot. Its higher expression is visualized in E13 cortical and thalamic extract.